Princeton Plasma Physics Laboratory

PPPL- 4290

PPPL- 4290

Lithium Surface Coatings for Improved Plasma Performance in NSTX

H.W. Kugel, M. G. Bell, J-W. Ahn, J.P. Allain, R. Bell , J. Boedo, C. Bush, D. Gates, T. Gray,S. Kaye, R. Kaita, B. LeBlanc, R. Maingi, R. Majeski, D. Mansfield, J. Menard, D. Mueller, M. Ono, S. Paul, R. Raman, A.L. Roquemore, P.W. Ross, S. Sabbagh, H. Schneider, C. H. Skinner, V. Soukhanovskii, T. Stevenson, J. Timberlake, W.R. Wampler, and L. Zakharov

February 2008

PPPL PRINCETON PLASMA PHYSICS LABORATORY

Prepared for the U.S. Department of Energy under Contract DE-AC02-76CH03073.

Princeton Plasma Physics Laboratory
Report Disclaimers

Full Legal Disclaimer

Trademark Disclaimer

PPPL Report Availability

Princeton Plasma Physics Laboratory:

http://www.pppl.gov/techreports.cfm

Office of Scientific and Technical Information (OSTI):

http://www.osti.gov/bridge

Related Links:

U.S. Department of Energy

Office of Scientific and Technical Information

Fusion Links

Lithium surface coatings for improved plasma performance in NSTX

H. W. Kugel [a], M. G. Bell [a], J-W. Ahn [b], J. P. Allain [g] R. Bell [a], J. Boedo [b], C. Bush [c], D. Gates [a], T. Gray [a],S. Kaye [a], R. Kaita [a], B. LeBlanc [a], R. Maingi [c,] R. Majeski [a], D. Mansfield [a], J. Menard [a], D. Mueller [a], M. Ono [a], S. Paul [a], R. Raman [d], A. L. Roquemore [a], P. W. Ross [a], S. Sabbagh[e], H. Schneider [a],C. H. Skinner [a], V. Soukhanovskii [f], T. Stevenson [a], J. Timberlake [a], , W. R. Wampler [h], L. Zakharov [a]

[a] Princeton Plasma Physics Laboratory, Princeton, NJ 08543
[b] University of California at San Diego, La Jolla, CA 92093
[c] Oak Ridge National Laboratory, Oak Ridge, TN 37831
[d] University of Washington, Seattle, WA 98195
[e] Columbia University, New York, NY 10027
[f] Lawrence Livermore National Laboratory, Livermore, CA 94551
[g] Purdue University, School of Nuclear Engineering, West Lafayette, IN 47907
[h] Sandia National Laboratories, Albuquerque, NM 87185

ABSTRACT

NSTX high-power divertor plasma experiments have shown, for the first time, significant and frequent benefits from lithium coatings applied to plasma facing components. Lithium pellet injection on NSTX introduced lithium pellets with masses 1 to 5 mg via He discharges. Lithium coatings have also been applied with an oven that directed a collimated stream of lithium vapor toward the graphite tiles of the lower center stack and divertor. Lithium depositions from a few mg to 1 g have been applied between discharges. Benefits from the lithium coating were sometimes, but not always seen. These improvements sometimes included decreases plasma density, inductive flux consumption, and ELM frequency, and increases in electron temperature, ion temperature, energy confinement and periods of MHD quiescence. In addition, reductions in lower divertor D, C, and O luminosity were measured.

Subject Categories: Lithium; Particle control; Wall conditioning; Wall pumping; Impurity control.

Keywords: C0600 Coatings; P0500 Plasma-materials interaction; S1300 Surface effects; I0100 Impurities.

PAC Numbers: 52.25.Vy; 52.40.-w; 52.40.Hf; 52.55.Fa.

I. INTRODUCTION

The National Spherical Torus Experiment [1] (NSTX) research on lithium-coated plasma facing components (PFC) is the latest step in a research program to develop liquid lithium for providing a self-healing plasma facing surface in a DT reactor. [2] The initial NSTX lithium research is aimed towards sustaining the current non-inductively in H-mode plasmas, which requires control of both secular density rises and impurity influxes. Motivated by the long range potential of lithium PFCs, NSTX has been investigating lithium coatings for density control and impurity control as part of a phased, three-part approach to lithium PFCs: first with lithium pellet injection, then with lithium evaporators, and finally with a liquid lithium divertor. This phased approach is allowing NSTX control systems, diagnostics, and research to be adapted to lithium-improved wall conditions. Under these conditions, deuterium ions and neutrals incident on solid lithium PFCs can react to form lithium deuteride (LiD), which remains in the lithium unavailable for recycling. This is in contrast to molecular deuterium, which is not gettered, and can recycle. This behavior of ions and neutrals provides a pumping effect over the plasma wetted area for a wide range in plasma density and shape, and this is the basis for the control of wall recycling and impurities being investigated in this work.

II. EXPERIMENT DESCRIPTION

NSTX capabilities presently include $R_0 \leq 0.85$ m, $a \leq 0.67$ m, $R/a \geq 1.26$, $k \leq 2.7$, $d \leq 0.8$, $I_p \leq 1.5$ MA, $B_T \leq 0.3$T, and 1.5 sec maximum pulse length. Copper passive stabilizer plates, graphite power handling surfaces, 7 MW of deuterium Neutral Beam heating, 6 MW of 30 MHz High Harmonic Fast Wave (HHFW) for heating and current drive at 10-20 ω_{ICRF} provide additional experimental versatility. The 0.2 m radius center stack (CS) is clad with alternating vertical columns of 1.3 cm thick graphite (Union Carbide, Type ATJ) tiles between columns of 2-D Carbon Fiber Composite (CFC) (Allied Signal, Type 865-19-4) tiles. The inner divertor tiles are 5.1 cm thick graphite; the outer divertor and passive stabilizer plate tiles are 2.5 cm thick graphite. The plasma facing components (PFCs) are conditioned as required using bakeout at 350°, He Glow Discharge Cleaning (HeGDC) and boronization. [3] A sabot-style Lithium Pellet Injector (LPI) can inject lithium, other low-Z pellets, or powders into edge plasmas. [4] The

NSTX configuration enables experiments with ohmic, neutral beam (NB), and high harmonic fast wave (HHFW) heated discharges on wall limiter start-up plasmas, lower single-null diverted plasmas, and double null diverted plasmas with and without coaxial helicity injection (CHI). [1] Fig. 1 shows a poloidal cross section of NSTX and the locations of the Lithium Evaporator (LITER) for the 2006 and 2007 aiming angles, and two Quartz Deposition Monitors (QDM).

Fig. 2 shows a schematic diagram of the LITER evaporator. The unit has a 90 g lithium capacity. It consists of a main reservoir oven and an output duct (snout) to allow insertion in an available gap in the upper divertor region. The 2006 version was aimed 22° downward at the lower shoulder of the center stack; the 2007 version was aimed about 12° downward toward the inner edge of the inner divertor as seen in Fig.1. Two heaters are used; one heater on the output duct and one heater on the main reservoir. The heater on the main reservoir is typically operated to provide liquid lithium temperatures of 600-680°C. The heater on the output duct is operated about 50-100°C hotter than the heater on the main reservoir to reduce lithium condensation on the output duct aperture. The evaporation rate is controlled by varying the oven temperature. Typical evaporation rates have been in the range 1 to 40 mg/min. Fig.3 shows the results of laboratory angular distribution measurements of the output lithium beam using a QDM indicating a gaussian half-width of approximately 7 cm at a distance of 30.2 cm. Fig. 4 shows a simulation of the lithium deposition in NSTX. [5]

III. EXPERIMENTAL RESULTS

A. LITHIUM PELLET INJECTION RESULTS

In NSTX, recycling of hydrogenic species from the plasma contact surfaces, contributes to a secular density rise observed in most H-mode, NB heated plasmas. Experiments on the Tokamak Fusion Test Reactor (TFTR) obtained reduced recycling and significantly enhanced performance using pellet injection, evaporation, and laser techniques to apply lithium to its graphite inner toroidal limiter, but only after it had been thoroughly degassed by repeated helium discharges. [6] This wall degassing is believed

to avoid the applied lithium from combining with the fuel gas embedded in the graphite PFCs. Lithium reactions with gas embedded in the graphite make it unavailable for pumping incident ions and neutrals. In 2005, LPI experiments in NSTX reproduced this recycling reduction. [7] First, the plasma facing surfaces were conditioned with a series of Helium discharges. Then one or two low velocity (~100m/s) lithium pellets with masses 2 – 5 mg were injected 1 each, or 2 each, into 10 to 20 repeated ohmic of helium discharges, to introduce a total of 24 to 30 mg of lithium on either the graphite center stack limiter or the lower divertor immediately. Spectroscopic data indicated that the injected lithium was deposited primarily on the surfaces surrounding the plasma contact area. In both the limiter (CS limited) and lower divertor, Lower Single Null (LSN) configurations, the first subsequent deuterium NB heated L-mode plasma showed a reduction in the volume-average plasma density during the NBI heating by a factor of about 2 compared with the respective reference discharge before the lithium deposition. This reduction in density was less on the next shot and was not evident on the third shot. This is illustrated in Fig. 5 for a Lower Single Null (LSN) divertor configuration L-mode plasma. The saturation of the apparent wall pumping can be understood if the effect occurs through the formation of LiD on the surface: the amount of lithium introduced could react with about 6–9 mg of deuterium, and about 3.5 mg of deuterium was injected on each discharge. The density in these discharges was chosen to be much less than typical L-mode discharges to provide a plasma particle content comparable to the available Li pumping capacity. Similar results were obtained with higher density H-mode plasmas, but without requiring the prior degassing of the wall using ohmic helium discharges. In this case, degassing the walls with HeGDC between discharges was sufficient. Additional work is needed to understand this difference in required wall degassing.

The NSTX results for the limiter plasmas are similar to the experience with lithium coating in TFTR [6] and with a liquid-lithium limiter in the Current Drive Experiment - Upgrade (CDX-U). [8] These present NSTX LPI experiments extended the potential benefits of lithium surface coating for plasma density control to divertor plasmas, and suggested that additional lithium deposition could increase plasma

density pumping and prolong its durations. This conjecture motivated the development of a lithium evaporator for performing routine lithium coating over a significant fraction of the plasma facing surfaces.

B. LITHIUM EVAPORATOR RESULTS

In 2006, lithium coatings were applied with LITER-2006 aimed as shown in Fig.1 to direct a collimated stream of lithium vapor toward the graphite tiles of the lower center stack and divertor. Lithium depositions from a few mg to ~1 g were applied between discharges. The relatively low thermal inertia of LITER-2006 allowed cool-down in about 30-60 mins, from temperatures (600-640°C) yielding relatively high evaporation rates (10-20 mg/min) to temperatures giving minimal evaporation (<375°C). This cool-down allowed opening diagnostic window shutters without risk of lithium coating of windows, and in addition, allowed HeGDC to be performed separately from the lithium evaporation. About 12 separate depositions of lithium were performed onto the lower divertor prior to D LSN NBI heated reference discharges. These individual depositions ranged from 1.6 mg to 4.8 g of lithium for a total of 9 g deposited by the end of the 2006 experimental campaign. This lithium amount would correspond to a thickness of 0.42 μm if averaged over the interior area of NSTX.

The initial lithium evaporations ranging from 1.6 mg to 643 mg employed no wall pre-conditioning with He ohmic discharges. Each of these lithium evaporations was followed by an L-mode D LSN reference discharge, which exhibited no improvement in plasma performance. This is consistent with the above pellet results, and expected if it is assumed that the deposited lithium reacted with the residual fuel gas embedded in the graphite PFCs. Motivated by these results, subsequent evaporations were preceded by 6 ohmic helium wall conditioning discharges of the same shape as the following L-mode LSN NBI reference discharge. In these cases, there were immediate frequent small decreases in the line-averaged n_e (*e.g.,* ~15%), and increases in the associated T_e, T_i, W_E, and τ_E. The wall conditioning aspect of this result is consistent with the 2005 LPI results for similar L-mode plasmas for which helium discharge conditioning was required prior to lithium deposition, for improvements in plasma performance.

Nevertheless, in spite of relatively large total lithium deposition ($\geq$ 600 mg), the improvement in plasma conditions reverted to the pre-lithium conditions by the following discharge.

The evaporations during the 2006 experimental campaign were used to test higher density H-mode reference discharges under lithium wall conditions. In these experiments, it was found that, contrary to the L-mode behavior, improvements in the higher density H-mode D reference plasma were observed without first preceding the discharge with Helium ohmic discharge conditioning. However, as before, however, these improvements in performance lasted for only about one discharge. This lack of need of Helium discharge preconditioning, contrary to previous L-mode results, suggested that NSTX H-mode edge conditions may be more sensitive than L-mode edge conditions to the beneficial effects of residual active lithium remaining on the unconditioned walls. The performance of D LSN H-mode NBI reference discharges following these evaporations occasionally exhibited improvements to the L-mode results described above. However, in order for improvement in performance, a minimum lithium deposition of about 600 mg was required. In addition, minimizing the duration between the end of the evaporation and the succeeding reference D discharge appeared to yield a more frequent improvement in performance. This can be understood as due to possible lithium reactions with the graphite substrate (*e.g.,* Li_2C_2 formation, intercalation, etc.) and components of the residual vacuum partial pressures *(e.g.*, H_2O, CO, CO_2). Longer term changes in performance included a reduction in Z_{eff} (r=0) due to reduced carbon in the core, which decreased as lithium recycling light deceased with discharge number, and a decrease in core oxygen light to levels at or below those directly following boronization. D_α luminosity was reduced by 70% during the 1st shot following a lithium deposition sequence, and if increased in subsequent discharges, but still remained lower than the levels in discharges without additional lithium deposition.

The 2006 results suggest that higher evaporation rates could provide depositions well above any erosion-related threshold, and that evaporating up to, and during discharges would minimize effects related to possible lithium reactions with the graphite

substrate and vacuum impurities. Therefore, LITER was upgraded in 2007 to increased capacity (91g vs 64 g), and reaimed toward the inner divertor for a threefold increase divertor target deposition. In addition, the output aperture area was increased by a factor of 1.7, and heater improvements made to allow higher evaporation rates. These changes increased the amount and rate of lithium deposited on the lower divertor target region during each deposition. Typical evaporation rates of 10 to 40 mg/min were tested for a total of lithium deposition of ~93 g by the end of the 2007 Experimental Campaign. This would correspond to a lithium thickness of 4.4 μm if averaged over the interior area of NSTX.

The 2006 LITER experiments deposited up to a factor of 40 more lithium (~1 g) before the succeeding reference D discharge than in the LPI experiments (25 mg), and the cumulative total was about a factor of 100 more lithium. The 2007 LITER experiments typically deposited about the same amount of lithium (~1g) before the succeeding reference D discharge, but provided continuous deposition between and during discharges. These changes yielded about the same level and frequency of improvements as in 2006. Fig.6 shows the 2007 database of electron stored energy (W_e) versus total stored energy (W_{MHD}) for all similar plasmas immediately following Li deposition, and for all similar discharges prior to the start of lithium depositions. Shown also are the averages and standard deviations of the two groups of points. It is seen that, on average, the total stored energy is higher after lithium deposition, and that this is mostly through an increase in electron stored energy. Fig. 7a shows the central electron temperature ($T_e(0)$) versus the volume averaged electron temperature <Te>. The central electron temperature ($T_e(0)$) shows no change but that <Te> increases after lithium deposition. Fig. 7b shows the central density ($n_e(0)$) versus the volume average electron density ($<n_e>$). There is a slight broadening of the electron density profile ($<n_e>$) after lithium deposition. Fig. 8 shows the central ion temperature $T_i(0)$ versus the volume average ion temperature $<T_i(0)>$ obtained by assuming the same density distribution (n_e) as the electrons. There is no evident effect on the temperatures after lithium deposition. Fig.s 9a and 9b compare examples of electron transport coefficients χ_e and ion transport coefficients χ_i derived using the time-dependent transport code

TRANSP. [9] They are for a quiescent interval in a discharge following Li deposition and the same interval in a discharge prior to lithium deposition. The edge χ_e and the core χ_i tend to decrease following lithium deposition consistent with a broadening of the profile. Fig. 10 shows significant D pumping at higher Li evaporation rates (35 mg/min). Prior to these discharges, typical lithium evaporation rates of 15 to 20 mg/min were used. A noteworthy observation during this work has been the influence of lithium wall conditions on ELM and MHD behavior. Fig.11 shows an example of the frequent reduction in ELM frequency and quiescent period following lithium deposition. It is seen in this example that after lithium deposition the stored energy W_{MHD} increased and the frequency of large ELMs was greatly reduced. Note the quiescent period exhibited in the edge D_α luminosity in the interval 0.3 to 0.8 s. With increasing lithium deposition on the PFCs, the edge D_α, CII, and O II luminosity decreased (Fig.12).

Typically, to facilitate plasma start-up conditions, HeGDC is applied between discharges for about 9 mins to remove near-surface molecular deuterium from the graphite walls prior to the next discharge. This practice was followed during the 2007 lithium experiments to condition graphite PFCs. Since LITER continued to evaporate during the HeGDC, this was effectively the process known as "lithiumization" (similar to boronization), whereby lithium atoms entering the HeGDC are ionized and deposited globally by the applied GDC bias (~400-600 v). While this lithiumization deposited lithium more globally, it also resulted in the codeposition of helium and lithium, which slowly outgassed during the subsequent deuterium discharge. This effect has been measured previously, and is attributed to helium trapping in solid lithium interstitial voids. [10] The subsequent outgassing is on the time scale of tens of minutes. Due to this trapped helium outgassing, the Helium luminosity increased with shot number as the total lithium deposition increased.

After venting the vessel to atmosphere, nuclear reaction analysis was performed to measure the concentration of D versus depth using $D(^3He,p)$ reactions and the concentration of lithium versus depth using $^7Li(p,\alpha)\alpha$ reactions on a poloidal array of graphite tiles through the lithium deposition vertical plane (Fig.13). The D coverage was

found to be in the range ~10^{17} to > 10^{19} D/cm^2, with the highest coverage (>10^{19} D/cm^2 extending to depths beyond the range of analysis, *i.e.*, >4 μm at the corner between the lower stack shoulder and the inner horizontal divertor. This was essentially the private flux region between the strike points for much of this work. Elsewhere, the D concentration was within 4 μm of the surface. The lithium coverage is present on all tiles the range from ~10^{17} to 10^{19} Li atoms/cm^2. The lithium coverage was ~10x lower on tiles in the lithium shadow provided by the center stack than on unshadowed tiles within line of sight from LITER at similar poloidal locations, and the D coverage was similar. This indicates that the D toroidal coverage was not greatly changed by lithium deposition. The deposited lithium was measured to be within 5 μm of the surface everywhere on the line-of-sight surfaces; on tiles with low coverage, the lithium was within 2 μm of the surface. This shows the lithium did not diffuse into the graphite beyond a few μm. This lithium appears to reside in a mixed concentration of presently unknown components; the possibility that these components could be carbon or oxygen is being investigated. X-ray Photoelectron Spectroscopy (XPS) was performed on surface region of some of the same divertor region tiles showed the presence C, O, B, and Li. XPS spectral line shifts along various points on the same tiles, and between adjacent tiles, indicated chemical changes that are under investigation. Lithium oxide formation (Li_2O) was not evident in the XPS spectra. A strong presence of lithium hydroxide (LiOH) and lithium carbonate (Li_2CO_3) was exhibited. A systematic experimental uncertainty was introduced in such measurements by the present need to remove the samples after venting the vessel, and thereby allowing atmospheric reactions with the sample surfaces to change the vacuum conditions. Work is in progress to determine the relative contributions of the effects of lithium interactions with the graphite, and the contributions to the residual vacuum partial pressures during the experimental campaign (e.g., H_2O, CO, CO_2), and exposure to atmosphere after the vessel venting.

IV. DISCUSSION

The behavior of ions and neutrals incident on solid Li to form LiD provides a pumping effect studied in this work. [11] In the case of lithium pellet injection into

diverted plasmas, the lithium is deposited toroidally along the plasma wetted region. In NSTX high triangularity diverted discharges with high flux expansion, this embodies the strike points and much of the inner and outer divertors. The lithium deposition, whether via injection into the deuterium shot of interest, or into preceding ohmic helium shots, can provide only a thin lithium layer. This is due to the inability of plasmas to accept more than a few mgs of injected lithium per discharge and remain unperturbed. Lithium evaporation from one evaporator prior to the discharge can provide lithium depositions on the divertor wetted region up x100 or more. This is thicker than what pellet injection provides, but with less than complete toroidal coverage unless several evaporators are used. The amount of incident deuterium ions and neutrals that can be pumped by a solid lithium coating on the plasma wetted area is determined by the depth range of the incident particles. At typical NSTX plasma energies, the range of deuterium is about 250 nm. [12] Yet, evaporated lithium depositions much thicker than this range appear to exhibit increased pumping as the thickness increased. This can be understood as due to the wings of the deposited lithium gaussian angular distribution, growing in thickness and extending the effective pumping area as the central the thickness increases. The rate of lithium deposition and the duration to the subsequent discharge appear to be important considerations. This can be understood if faster rates minimize the time allowed for lithium to react with the graphite substrate (*e.g.,* to form Li_2C_2 or inward diffusion [13]) and also minimize the time to react with the contributions of partial vacuum pressures (*e.g.*, H_2O, D_2O, CO, CO_2). These effects would reduce the amount of fresh atomic lithium available to form LiD with the incident D efflux.

The application of HeGDC during lithium evaporation to facilitate plasma start-up conditions results in a previously measured codeposition uptake of helium, at a rate of $1.6x10^{14}$ He atom /cm^2/s to average atomic ratios of He/Li ~0.008 in the resultant co-deposits. [10] The slow outgassing of this co-deposited helium relative to the duty cycle allows for accumulation and the observed increase of helium in D discharges with increasing discharge number. Future experiments will investigate the merits of possibly eliminating the need for this HeGDC by increasing the lithium deposition sufficiently to cover the D_2 from the preceding discharge.

The effect on plasma pumping and performance of injected lithium pellets and lithium evaporated coatings applied immediately prior to the reference shot exhibited some improvements. The improvements included *decreases* in plasma density, inductive flux consumption, and ELM frequency, and *increases* in electron temperature, ion temperature, energy confinement, and quiescent time. The work still in progress includes investigation of the origin of the continued secular density rise, (*i.e.,* small initial decrease in n_e, followed by a secular rise), the nature and duration of the lithium coatings, the reduction in ELM frequency and periods of quiescence, helium retention following HeGDC (and perhaps eliminating HeGDC), diagnostic window depositions, and operational issues with improved confinement (*e.g.,* increasing impurity confinement and core impurity radiation with discharge duration). In conclusion, while additional work is required to resolve the issues encountered, the NSTX high-power divertor plasma experiments have shown, for the first time, significant benefits from lithium coatings applied to plasma facing components.

ACKNOWLEDGMENTS

We acknowledge the technical contributions of S. Jurczynski, T.Provost, L.Guttadora, J. Taylor, S. Gifford, J. Desandro, J. Kukon, T. Czeizinger, J. Winston, L. Gernhardt, and P.Sichta. This work is supported by United States Department of Energy (US DOE) Contracts DE-AC02-76CH03073 (PPPL), DE-AC05-00OR22725 (ORNL), and those of Lawrence Livermore National Laboratory in part under Contract W-7405-Eng-48 and in part under Contract DE-AC52-07NA27344, and that of Sandia a multi-program laboratory operated by Lockheed Martin Company, for the United States Department of Energy's National Nuclear Security Administration under contract DE-AC04-94AL85000.

REFERENCES

1. M. G. Bell, *et al*., Nucl. Fusion **46 (8),** S 565 (2006), and references therein.

2. Fus. Eng. Design **72** 1-326 (2004). A large section of the “Special Issue on Innovative High-Power Density Concepts for Fusion Plasma Chambers” highlighted progress in this effort, and it continues as a primary focus of the USDOE "Advanced Limiter/Divertor Plasma-Facing Components (ALPS) program.

3. H. W. Kugel, *et al***.,** J. Nucl. Mater., **337-339,** 495 (2005).

4. G. Gettelfinger, *et al, Proc. 20th IEEE/NPSS Symposium on Fusion Engineering*, 359, San Diego CA, USA, 14–17 October 2003 (Piscataway NJ: IEEE).

5. L. E. Zakharov, PPPL Report PPPL-4187, Nov. 2006, Princeton Plasma Physics Laboratory, Princeton University, *unpublished*.

6. D. K. Mansfield, *et al*., Nucl. Fus., **41,** 1823 (2001).

7. H. W. Kugel, *et al*, J. Nucl. Mater., **363-365**, 791 (2007).

8. R. Majeski *et al.,* Nucl. Fusion, **45,** 519 (2005).

9. R.J. Hawryluk, in Physics of Plasmas Close to Thermonuclear Conditions, ed. by B. Coppi, et al.,(CEC, Brussels, 1980), Vol. 1, pp. 19-46.

10. Y. Hirooka, et al., J. Nucl. Mater., **363-365**, 775 (2007).

11. M. J. Baldwin, et al., Nucl. Fusion, **42**, 1318 (2002).

12. J. Brooks, et al., J. Nucl. Mater., **337-339**, 1053 (2005).

13. N. Itou, et al., J. Nucl. Mater., **290-293**, 281 (2001).

FIGURE CAPTIONS

Fig.1. Poloidal cross section of NSTX and the locations of the LIThium EvaporatoR (LITER) and the two Quartz Deposition Monitors (QDM). Shown are the LITER aiming angles used for the 2006 and 2007 experimental campaigns.

Fig. 2. Schematic diagram of the LITER evaporator.

Fig. 3. The results of a typical laboratory angular distribution measurement of the output lithium beam using a scanning QDM.

Fig.4. Simulation of the evaporated lithium distribution over the NSTX lower diivertor region.

.Fig. 5. A reduction in the volume-average density by a factor of about two was exhibited by Lower Single Null divertor NBI discharges following deposition of 25 mg of lithium using repeated Lithium Pellet Injection (LPI) into ohmic helium discharges

Fig. 6. The 2007 database of electron stored energy (W_e) versus total stored energy (W_{MHD}) for all similar plasmas immediately following lithium deposition, and for all similar discharges prior to lithium depositions.

Fig. 7a. The central electron temperature ($T_e(0)$) versus the volume averaged electron temperature <Te>. Fig. 7b. The central density ($n_e(0)$) *versus* the volume average electron density ($<n_e>$).

Fig. 8. The central ion temperature $T_i(0)$ versus the volume average ion temperature $<T_i(0)>$ obtained by assuming the same density distribution (n_e) as the electrons.

Fig. 9a and 9b. Comparison of examples of electron transport coefficients χ_e and ion transport coefficients, and χ_i derived respectively using the time dependent transport

code TRANSP for a quiescent interval in a discharge following lithium deposition with the same interval in a prior to lithium deposition discharge.

Fig. 10. Significant D pumping at higher Li evaporation rates (35 mg/min). Prior to these discharges, typical lithium evaporation rates of 15-20 mg/min were used.

Fig.11. A frequent reduction in ELM frequency and quiescent period following lithium deposition was observed. After lithium deposition the stored energy W_{MHD} increased and the frequency of large ELMs was greatly reduced. Note the quiescent period exhibited in the edge Dα luminosity in the interval 0.3-0.8 s.

Fig. 12. The lower divertor D_α, C II, and O II luminosity decreased with increasing lithium deposition on PFCs.

Fig.13. Average coverage of Li & D on each measured graphite tile after the 2006 Experimental Campaign. Tiles shadowed by the Center stack have ~ 10x less lithium than unshadowed tiles, whereas D coverage is similar.

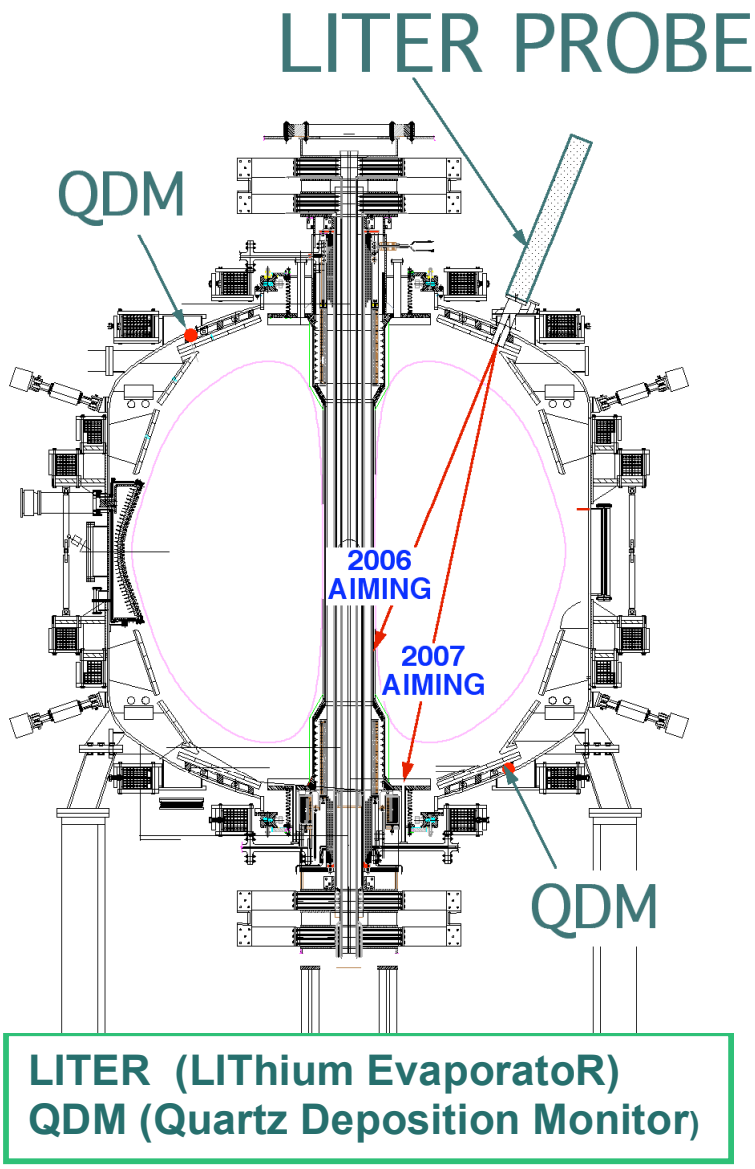

Fig.1. Poloidal cross section of NSTX and the locations of the LIThium EvaporatoR (LITER) and the two Quartz Deposition Monitors (QDM). Shown are the LITER aiming angles used for the 2006 and 2007 experimental campaigns.

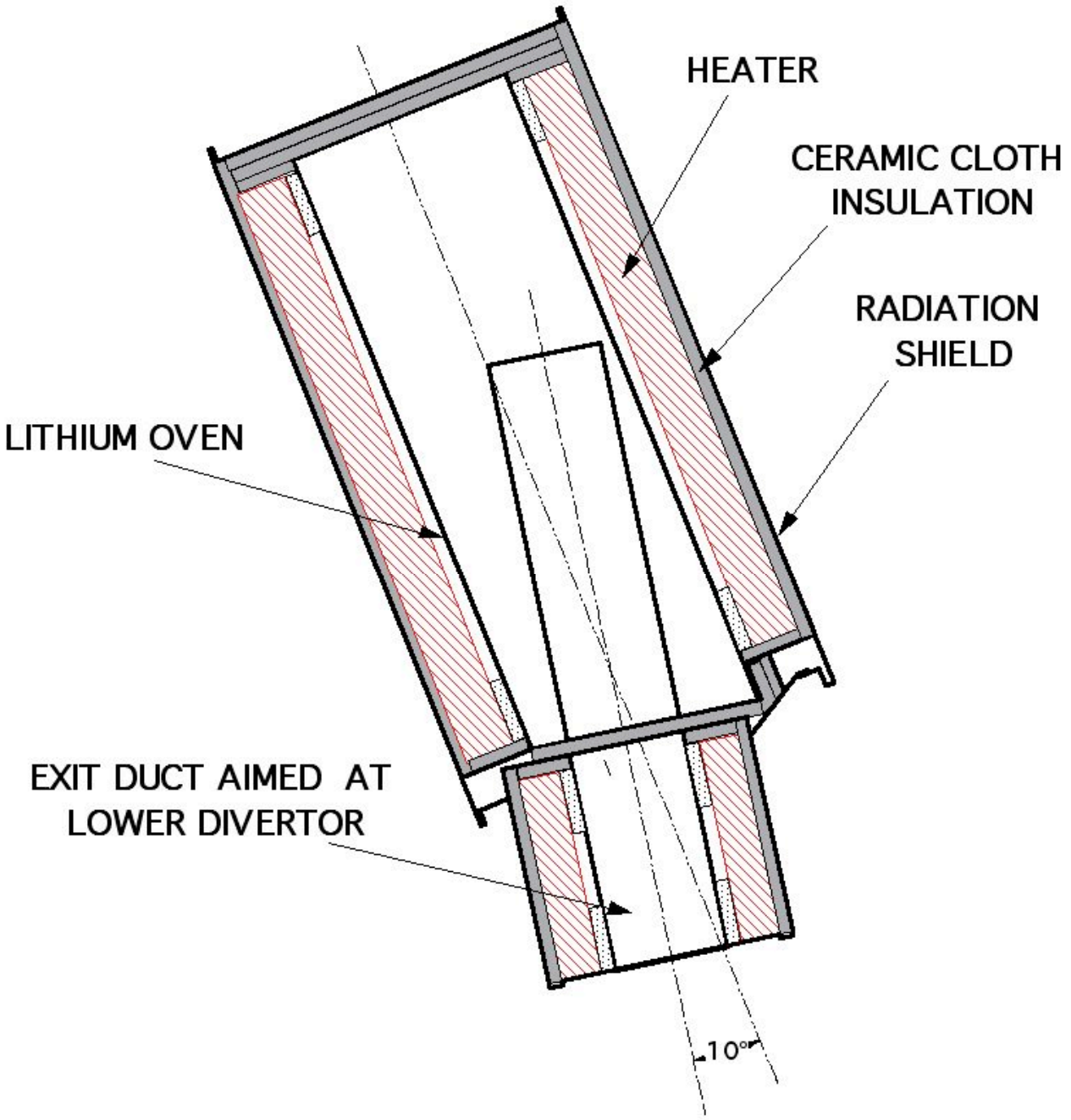

Fig. 2. Schematic diagram of the Lithium Evaporator (LITER 2007).

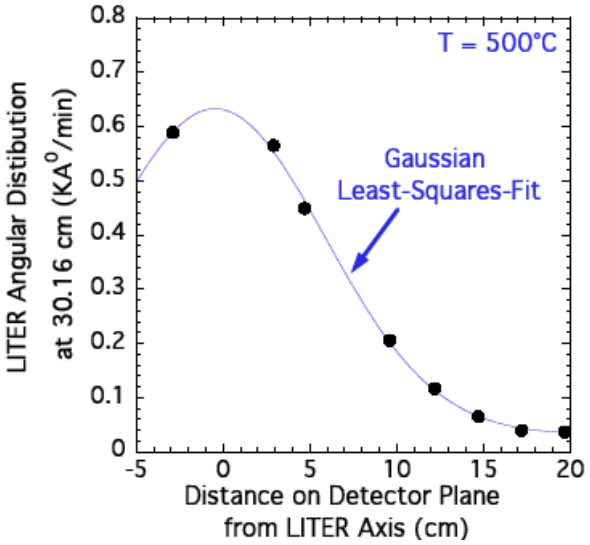

Fig.3. The results of a typical laboratory angular distribution measurement of the output lithium beam using a scanning QDM.

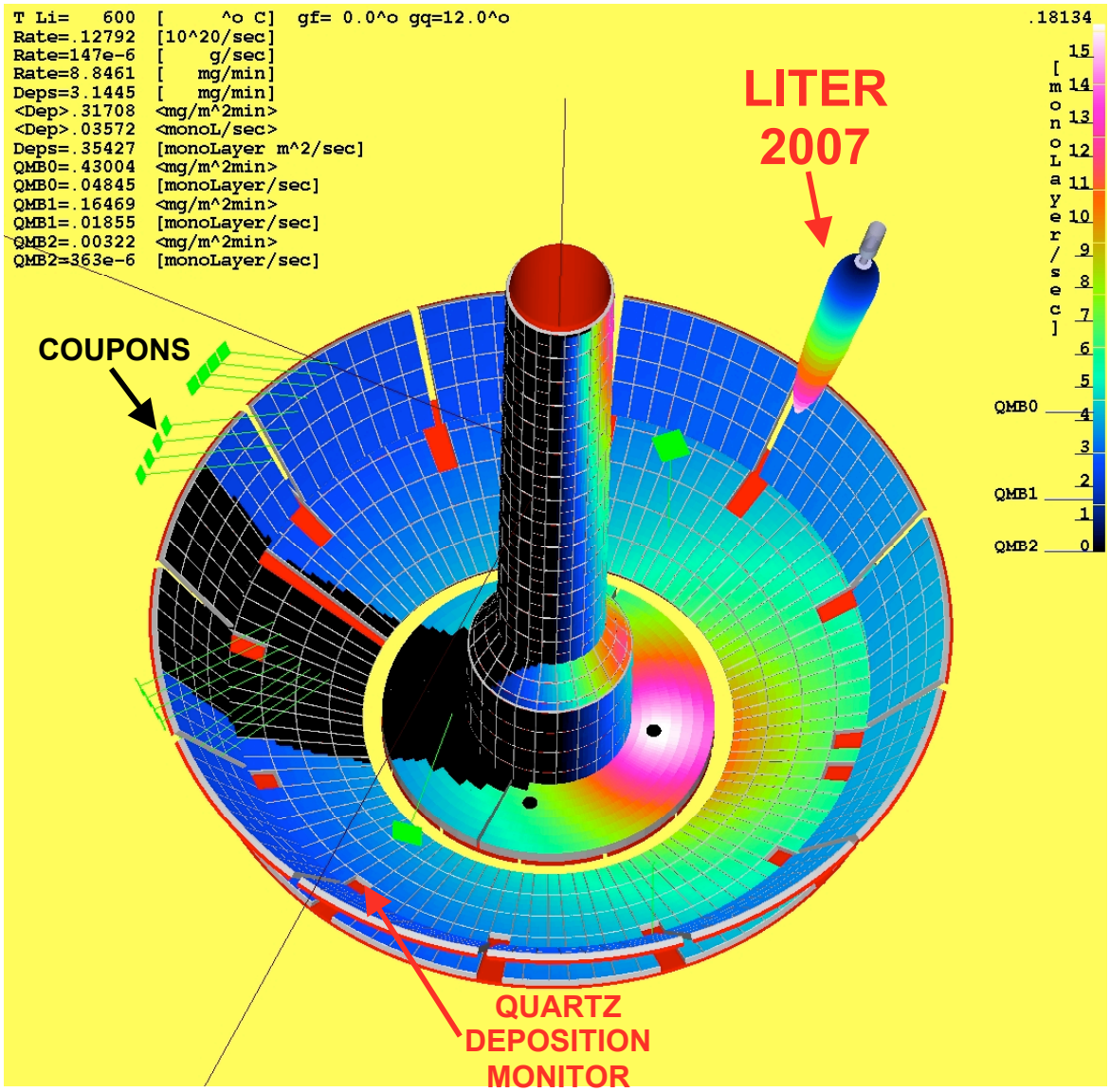

Fig.4. Simulation of the evaporated lithium distribution over the NSTX lower diivertor region.

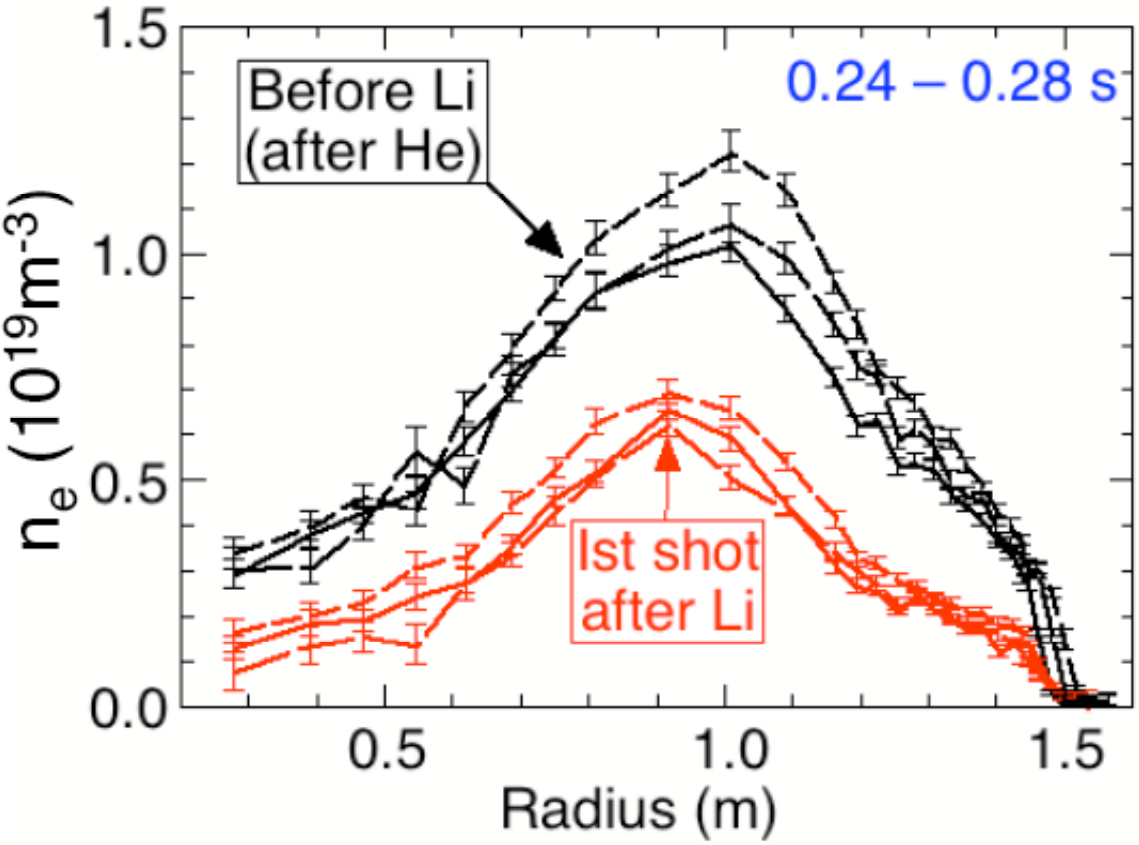

Fig. 5. A reduction in the volume-average density by a factor of about two was exhibited by Lower Single Null divertor NBI discharges following deposition of 25 mg of lithium using repeated Lithium Pellet Injection (LPI) into ohmic helium discharges

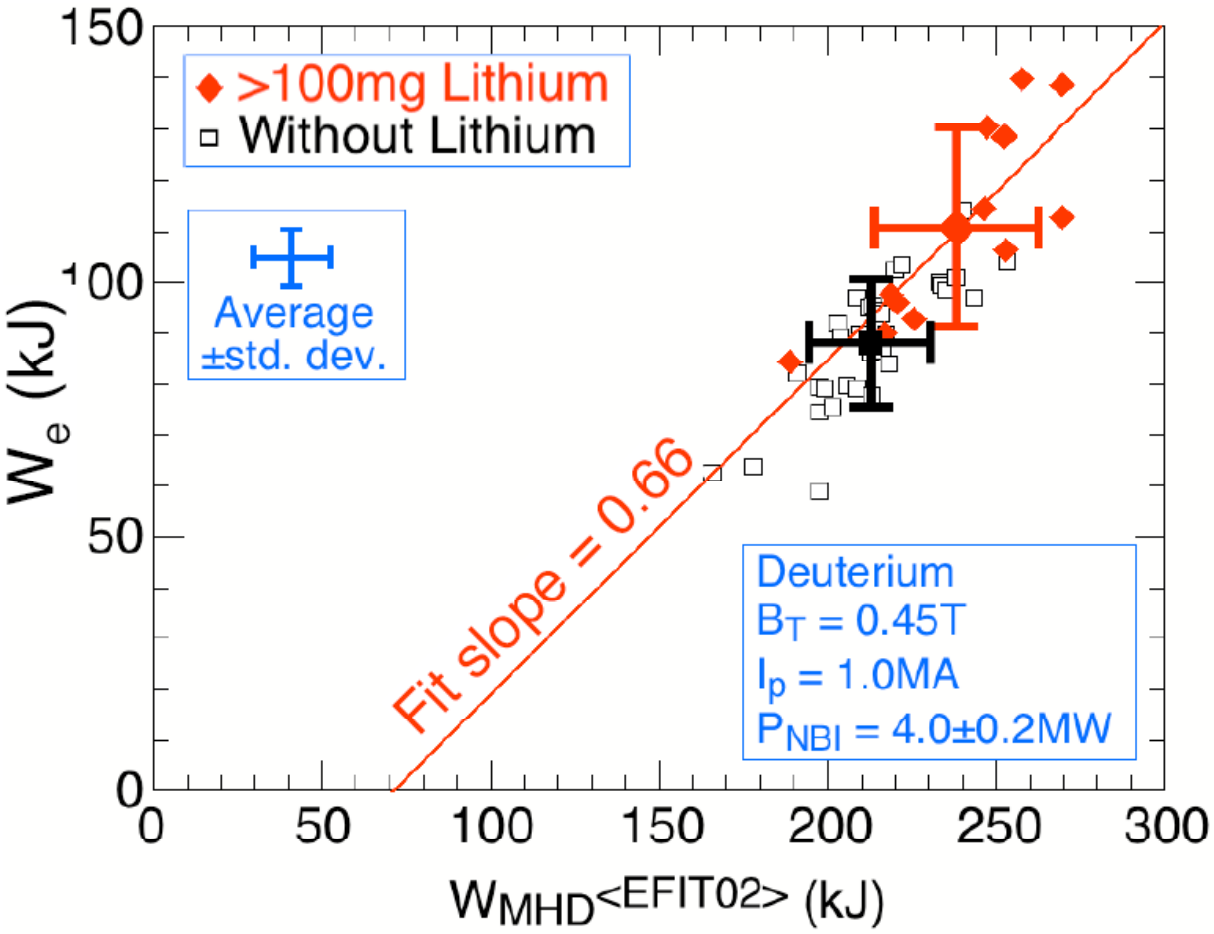

Fig. 6 The 2007 database of electron stored energy (W_e) versus total stored energy (W_{MHD}) for all similar plasmas immediately following lithium deposition, and for all similar discharges prior to lithium depositions.

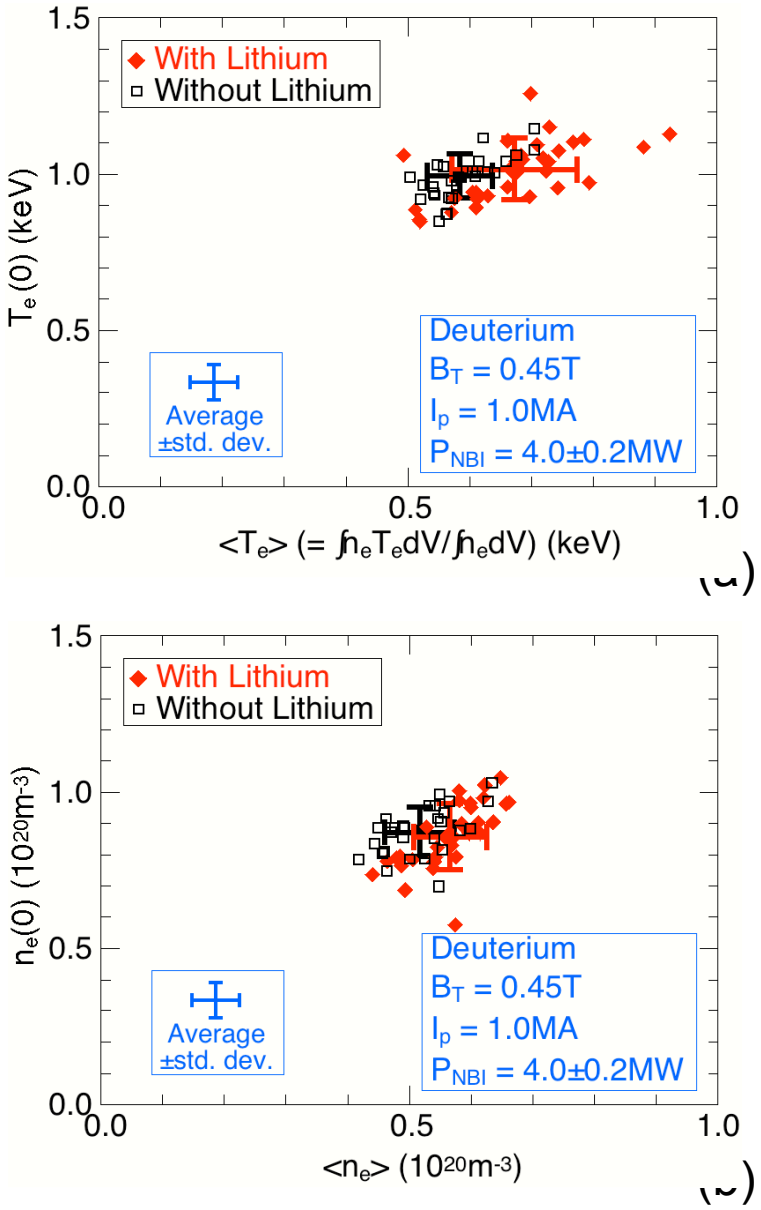

Fig. 7a The central electron temperature ($T_e(0)$) versus the volume averaged electron temperature <Te>. Fig. 7b The central density ($n_e(0)$) versus the volume average electron density (<n_e>).

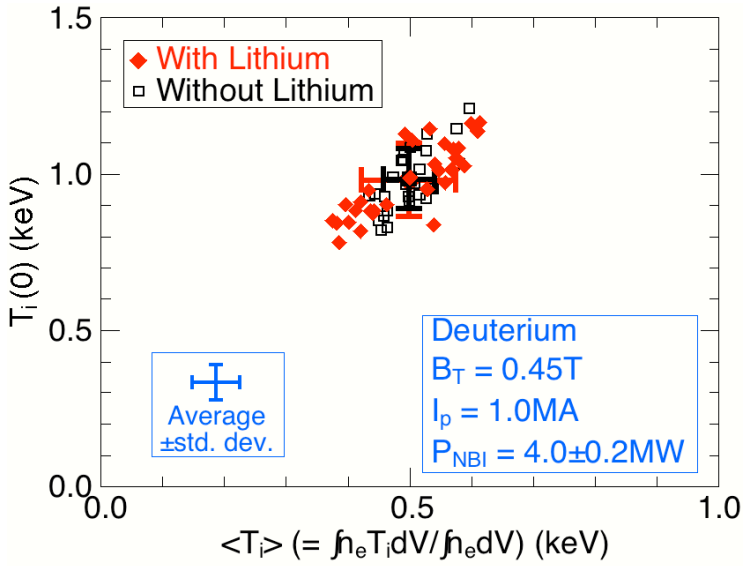

Fig. 8. The central ion temperature $T_i(0)$ versus the volume average ion temperature $\langle T_i(0) \rangle$ obtained by assuming the same density distribution (n_e) as the electrons.

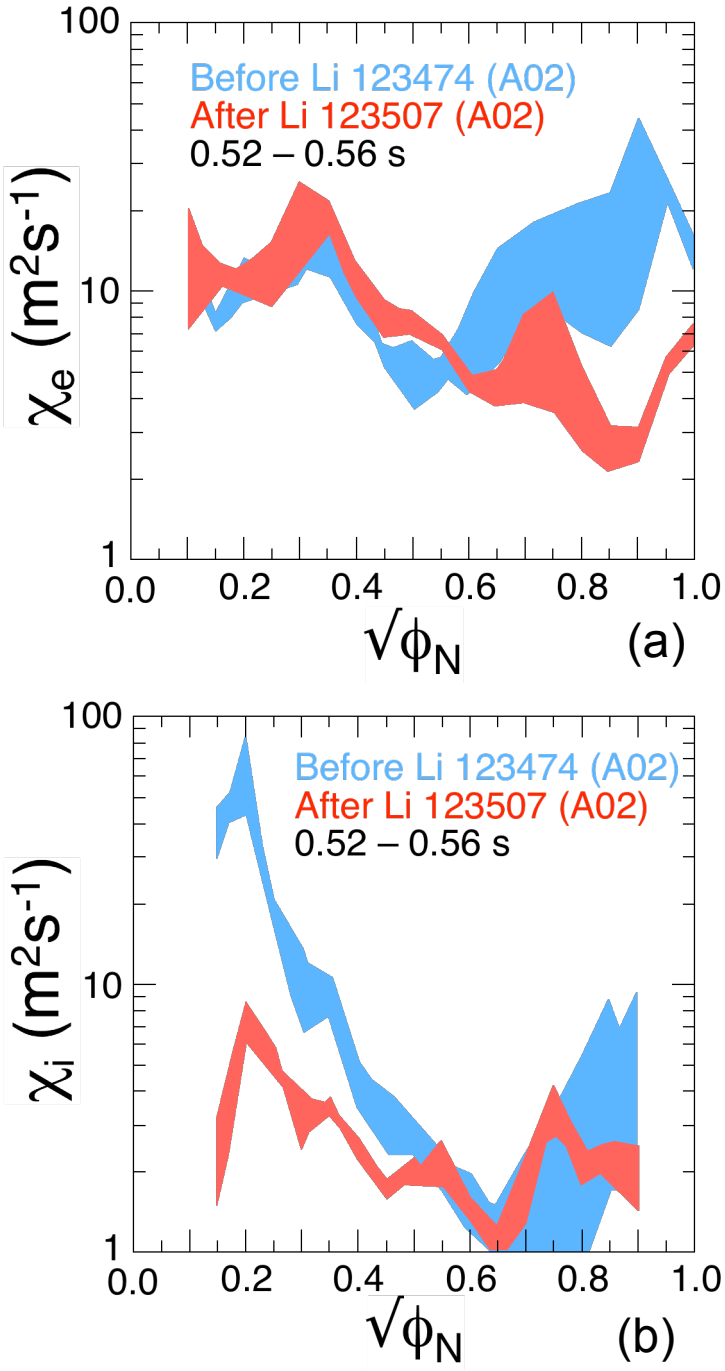

Fig. 9a and 9b. Comparison of examples of electron transport coefficients χ_e and ion transport coefficients, and χ_i derived respectively using the time dependent transport code TRANSP for a quiescent interval in a discharge following lithium deposition with the same interval in a prior to lithium deposition discharge.

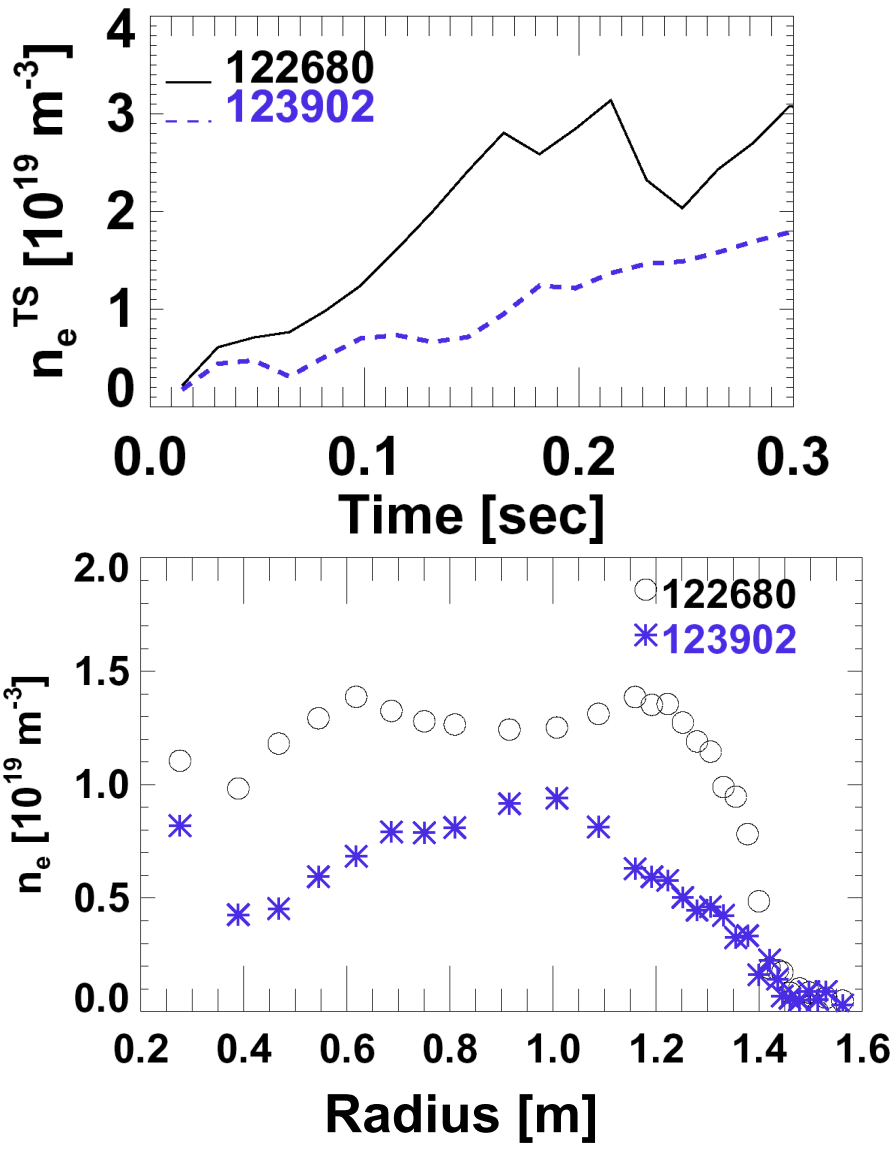

Fig. 10 Significant D pumping at higher Li evaporation rates (35 mg/min). Prior to these discharges, typical lithium evaporation rates of 15-20 mg/min were used.

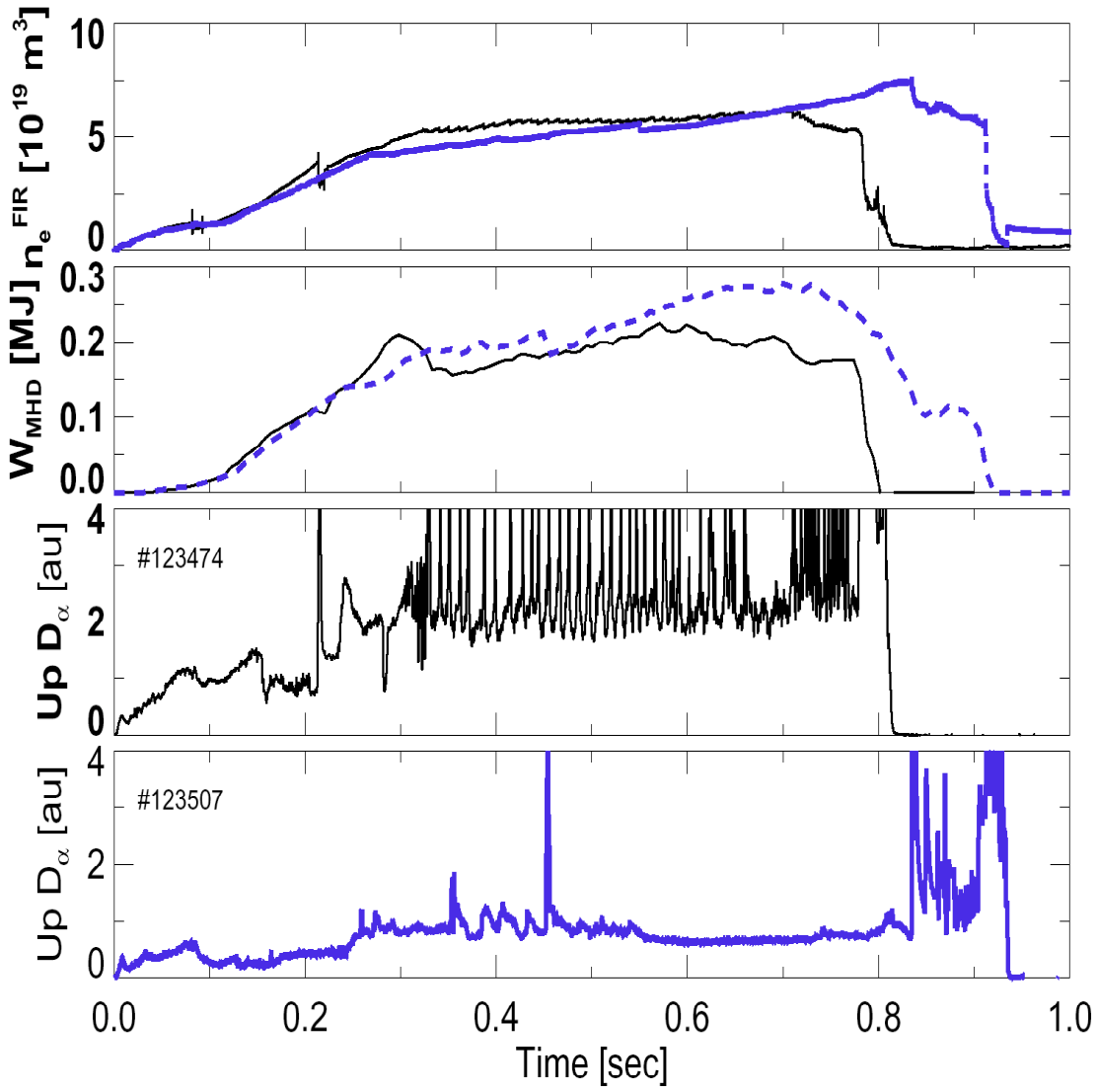

Fig.11 A frequent reduction in ELM frequency and quiescent period following lithium deposition was observed. After lithium deposition the stored energy W_{MHD} increased and the frequency of large ELMs was greatly reduced. Note the quiescent period exhibited in the edge Dα luminosity in the interval 0.3-0.8 s.

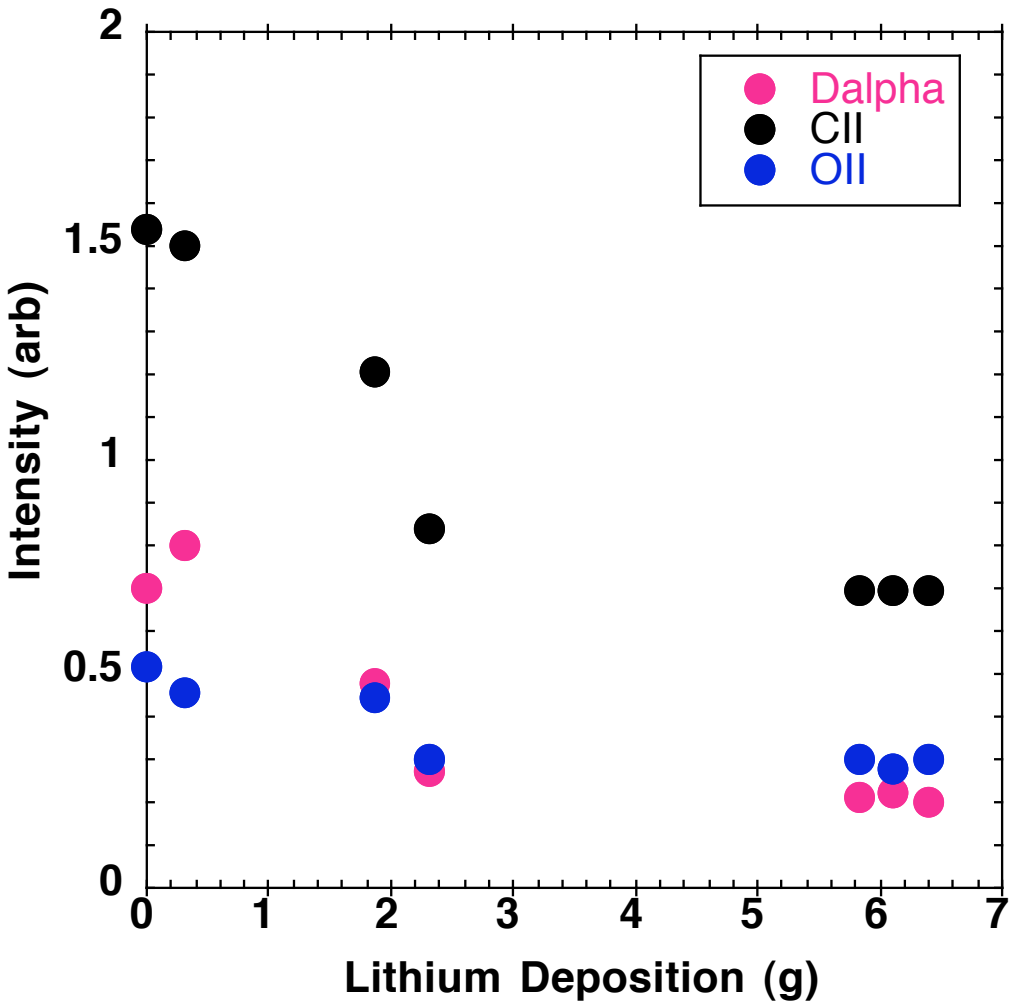

Fig. 12. The lower divertor D_α, C II, and O II luminosity decreased with increasing lithium deposition on PFCs.

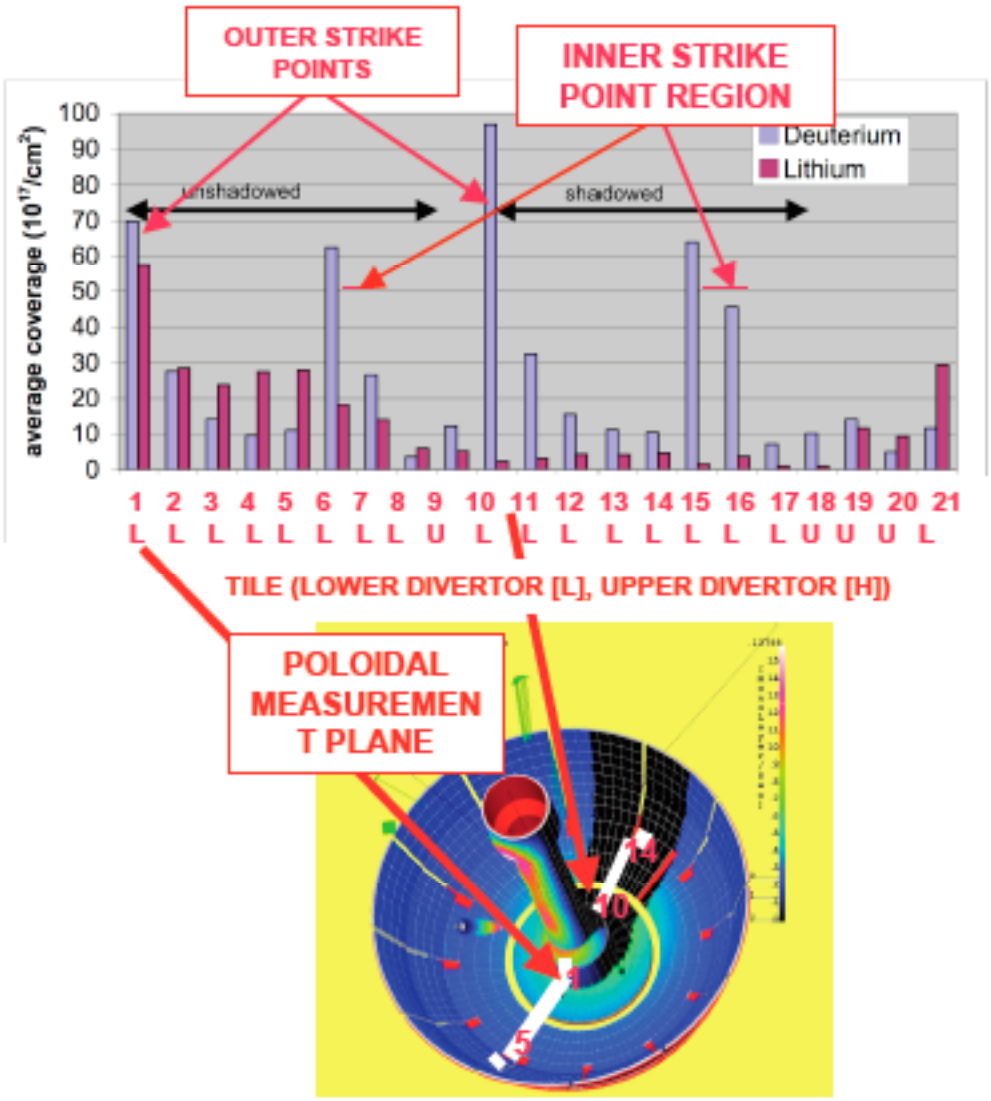

Fig.13. Average coverage of Li & D on each measured graphite tile after the 2006 Experimental Campaign. Tiles shadowed by the Center stack have ~ 10x less lithium than unshadowed tiles, whereas D coverage is similar.

The Princeton Plasma Physics Laboratory is operated
by Princeton University under contract
with the U.S. Department of Energy.

Information Services
Princeton Plasma Physics Laboratory
P.O. Box 451
Princeton, NJ 08543

Phone: 609-243-2750
Fax: 609-243-2751
e-mail: pppl_info@pppl.gov
Internet Address: http://www.pppl.gov